Influence of water and sediment supply on the stratigraphic record of alluvial fans and deltas: Process controls on stratigraphic completeness

Kyle M. Straub[1] and Christopher R. Esposito[1]

Received 14 November 2012; revised 9 March 2013; accepted 14 March 2013.

[1] Stratigraphy contains the most complete record of information necessary to quantitatively reconstruct paleolandscape dynamics, but this record contains significant gaps over a range of time and space scales. These gaps result from stasis on geomorphic surfaces and erosional events that remove previously deposited sediment. Building on earlier statistical studies, we examine stratigraphic completeness in three laboratory experiments where the topography of aggrading deltas was monitored at high temporal and spatial scales. The three experiments cover unique combinations in the absolute magnitudes of sediment and water discharge in addition to generation of accommodation space through base-level rise. This analysis centers on three time scales: (1) the time at which a record is discretized (t), (2) the time necessary to build a deposit with mean thickness equivalent to the maximum roughness on a surface (T_c), and (3) the time necessary for channelized flow to migrate over all locations in a basin (T_{ch}). These time scales incorporate information pertaining to the time-variant topography of actively changing surfaces, kinematics by which the surfaces are changing, and net deposition rate. We find that stratigraphic completeness increases as a function of t/T_c but decreases as a function of T_c/T_{ch} over the parameter space covered in the experiments. Our results suggest that environmental signals disconnected from a sediment routing system are best preserved in systems with low T_c values. Nondimensionalizing t by T_c, however, shows that preservation of information characterizing system morphodynamics is best preserved in stratigraphy constructed by systems with low water to sediment flux ratios.

Citation: Straub, K. M., and C. R. Esposito (2013), Influence of water and sediment supply on the stratigraphic record of alluvial fans and deltas: Process controls on stratigraphic completeness, *J. Geophys. Res. Earth Surf. 118*, doi:10.1002/jgrf.20061.

1. Introduction

[2] In a seminal publication on the completeness of the stratigraphic record, *Ager* [1973] elegantly stated that stratigraphy is "more gap than record." By this statement, Ager meant that time periods of nondeposition and erosion combine in all environments over a range of time and space scales to produce a record that is fundamentally constructed of snippets of environmental information recorded in short burst of deposition. To demonstrate the fraction of time represented in even the most complete stratigraphic records, Ager noted that deposition in deep-marine settings with little sediment reworking coupled with high hemipelagic fallout leads to deposition rates of at most a third of a millimeter per year. Given sediment grain sizes on the order of 1 μm, this rate would suggest the deposition of at most one grain of sediment per day. Depending on the time resolution of a record one requires, an investigator might view this as incredibly continuous or discontinuous sedimentation, and this is possibly the best case scenario. In environments with frequent alterations between erosion and deposition over a range of time scales, for example deltas, stratigraphic completeness can be far less [*Jerolmack and Sadler*, 2007]. This led *Ager* [1973] to note that in discussions of continuous sedimentation, one should note the temporal resolution over which they are referring, an argument made quantitatively by *Strauss and Sadler* [1989].

[3] While it is true that at many scales the stratigraphic record contains significant temporal gaps, it is also true that alluvial basins contain the most complete record of information necessary to quantitatively reconstruct paleolandscape dynamics for the majority of Earth History [*Ager*, 1973; *Allen and Allen*, 1990; *Paola*, 2000]. As such, developing methods for quantifying stratigraphic completeness is critical for constraining the precision of information we hope to extract. For example, changes in solar insolation (e.g., Milankovitch cycles) have been hypothesized to produce cyclic variations in precipitation, sediment supply, and sea level over geological time. To more fully understand the influence of Milankovitch cycles on these environmental variables, a suite of studies has

[1]Department of Earth and Environmental Sciences, Tulane University, New Orleans, Louisiana, USA.

Corresponding author: K. M. Straub, Department of Earth and Environmental Sciences, Tulane University, New Orleans, LA 70118, USA. (kmstraub@tulane.edu)

2169-9003/13/10.1002/jgrf.20061

searched for the signature of cycles in stratigraphy. These field studies cover a range of geological settings from deep-marine sites dominated by hemipelagic fallout [*Hinnov*, 2000; *Aziz et al*., 2008a] to deltaic stratigraphy in continental interior settings [*Aziz et al*., 2008b; *Abels et al*., 2010]. The accurate identification of Milankovitch cycles in stratigraphy requires deposits that record time at a precision significantly below the signal frequency, such that statistical tests can be performed to rule out null hypotheses [*Jerolmack and Paola*, 2010; *Meyers*, 2012]. This line of thought holds for other temporal signals we hope to extract from stratigraphy, both cyclic and noncyclic in nature. In this work, we limit our discussion of the stratigraphic record to how time is stored in channelized deposits.

[4] Manuscripts by *Strauss and Sadler* [1989] and *Sadler and Strauss* [1990] were perhaps the first to develop quantitative theory for estimation of stratigraphic completeness. Their work used empirical measurements of stratigraphic completeness constructed from a global compilation of deposition rates in addition to stochastic and deterministic models of deposition. They concluded that stratigraphic completeness is correlated to the time scale at which a record is sampled, t, and long-term accumulation rate but is inversely correlated to the age of a section and the unsteadiness of the sedimentation rate. Importantly, while the stochastic and deterministic models presented in these works convincingly illustrate the influence of the above-mentioned parameters, they lack a direct connection to process (physics)-based controls on generation of stratigraphy. Thus, our goal here is to build upon the theory of *Strauss and Sadler* [1989] and *Sadler and Strauss* [1990] by linking changes in basin boundary conditions, specifically input water and sediment flux and subsidence rate, to stratigraphic completeness in deltaic environments.

[5] Unsteadiness in deposition rates arises from a range of forcings and processes. In all environments, allogenic forcings and autogenic processes interact to result in a quasi-stochastic distribution of sedimentation (and erosion) rates over all temporal and spatial scales [*Sadler*, 1981; *Gardner et al*., 1987; *Schumer and Jerolmack*, 2009; *Hajek et al*., 2010; *Wang et al*., 2011]. In addition to long discussed allogenic forcings, the last 10 years have witnessed an enhanced appreciation for the range of time and space scales over which autogenic processes operate. Recent work demonstrates that autogenic processes acting over long time scales control the evenness or unsteadiness with which basins fill [*Kim and Paola*, 2007; *Straub et al*., 2009]. These fluctuations in sediment transport are controlled by inherent characteristics of sedimentary systems, including channel mobility [*Hickson et al*., 2005; *Hoyal and Sheets*, 2009; *Van Dijk et al*., 2009], characteristic avulsion frequency [*Aslan et al*., 2005; *Jerolmack and Paola*, 2007; *Reitz et al*., 2010], sediment cohesion [*Hoyal and Sheets*, 2009], and tectonic environment [*Kim and Paola*, 2007]. As a result, even in environments where allogenic forcings are constant, significant temporal gaps in stratigraphic columns (i.e., measured sections, cores, logs) should be expected.

[6] Many of the questions outlined above have recently been explored using physical experiments. For example, several experiments have investigated the chronostratigraphic significance of surfaces formed during the evolution of deltas built from braided channels [*Van Heijst and Postma*, 2001; *Sheets et al*., 2007; *Strong and Paola*, 2008]. In these "noncohesive" channelized experiments, both allogenic and autogenic variation in transport conditions resulted in stratigraphic surfaces that were the amalgamation of many time surfaces. This observation has also been noted in several numerical models and field studies [*Catuneanu et al*., 1998; *Holbrook*, 2001; *Blum and Aslan*, 2006]. In several recent fluvio-deltaic experiments, detailed measurements of evolving surfaces have been made in order to characterize topographic attributes [*Edmonds et al*., 2009; *Martin et al*., 2009]. However, with the exception of a noncohesive channelized experiment (experiment: DB-03) performed at Saint Anthony Falls Laboratory and analyzed by *Sheets et al*. [2007], *Straub et al*. [2009], *Hajek et al*. [2010], *Ganti et al*. [2011], and *Straub et al*. [2012], no experiments have been performed which monitor topography at temporal resolutions necessary to quantify individual channel dynamics and relate these dynamics to how time is stored in stratigraphy.

[7] In this paper, we use data from three physical fluvial-deltaic experiments experiencing relative subsidence in an experimental basin to characterize the statistics associated with fluvial dynamics and geomorphic surface topography. We then relate these statistics to stratigraphic time completeness over a range of scales and compare statistics characterizing the stratigraphic surfaces to geomorphic surfaces. The three experiments vary in the magnitude of input water and sediment discharge (Q_w and Q_s, respectively) and in the ratio of Q_w:Q_s. We choose to examine the influence of Q_w and Q_s in addition to their relative ratio as several recent studies note that these parameters influence autogenic time scales and the lateral mobility of transport systems [*Clarke et al*., 2010; *Kim et al*., 2010; *Powell et al*., 2012]. We also choose to examine stratigraphic completeness resulting from experiments with constant boundary conditions (i.e., isolating autogenic dynamics and thus ignoring systems with changing allogenic forcings). This is done as a first step in an exploration of process controls on stratigraphic completeness, with the hope that understanding systems with constant boundary conditions will aid in future analysis of systems with complex forcings.

2. Experimental Methods

[8] To examine the influence of Q_w and Q_s and their relative ratio on the completeness of deltaic stratigraphy, we performed three laboratory experiments. In the last decade, a wide variety of studies have investigated the surface dynamics and stratigraphy associated with channelized deltas at reduced scale [*Sheets et al*., 2002; *Kim et al*., 2006; *Hoyal and Sheets*, 2009; *Van Dijk et al*., 2009; *Reitz et al*., 2010; *Powell et al*., 2012]. As outlined in a recent review by *Paola et al*. [2009], these experiments produce spatial structure and kinematics that, although imperfect, compare well with natural systems despite differences of spatial scale, time scale, material properties, and number of active processes. As a result, these experiments provide morphodynamic and stratigraphic insight into the evolution of channelized settings under an array of external and internal influences. While many challenges exist in directly upscaling experimental results, several recent studies demonstrate that utilization of appropriate statistical tools allows for the comparison of laboratory and field stratigraphy [*Straub et al*., 2009; *Hajek et al*., 2010; *Wang et al*., 2011].

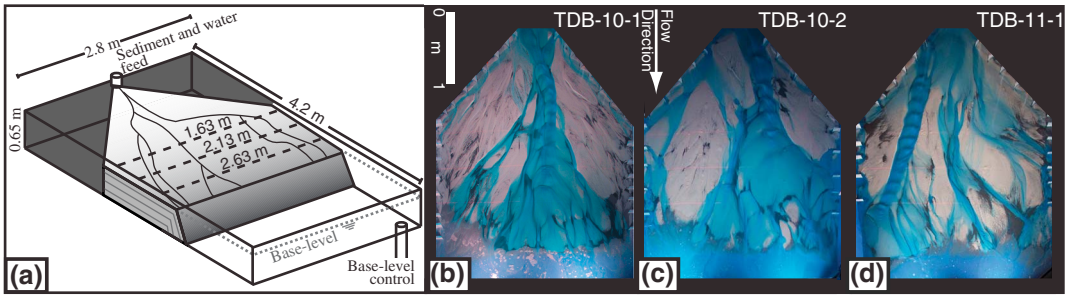

Figure 1. (a) Schematic diagram of Tulane Delta Basin facility. Positions of topographic transects are indicated by black dashed lines on fluvial surface. Note base-level control is in opposite corner of basin from infeed point. (b, c, and d) Photographs of active delta tops during TDB-10-1, TDB-10-2, and TDB-11-1, respectively.

[9] The three experiments performed in this study were conducted in the Delta Basin at Tulane University's Sediment Dynamics Laboratory (Figure 1). This basin is 2.8 m wide by 4.2 m long and 0.65 m deep. Accommodation is created in the Delta Basin by slowly increasing base level using a motorized weir that is in hydraulic communication with the basin. This system allows base-level control through a computer interface with submillimeter-scale resolution. Water and sediment supply to the basin are also controlled through the above-mentioned computer interface.

[10] All experiments included an initial build out phase in which sediment and water were mixed in a funnel and fed from a single point source at the center of the upstream wall. After a system prograded 3.1 m from the source to shoreline, base-level rise was initiated at a rate equal to the total sediment discharge divided by the desired delta-top area. In each experiment, the combination of sediment feed rate and base-level rise allowed the shoreline to be maintained at an approximately constant location through the course of the experiment.

[11] The three experiments had unique combinations of input Q_w and Q_s and base-level rise rate (Table 1). The first experiment, TDB-10-1, acted as the control experiment for the study and had input Q_w and Q_s and base-level rise rate ($\bar{r}$) of 0.011 L/s, 0.451 L/s, and, 5 mm/h, respectively. As such, Q_w:Q_s in this experiment was 41:1. In the second experiment, TDB-10-2, we doubled Q_w, Q_s and $\bar{r}$ relative to TDB-10-1. As both Q_w and Q_s were doubled relative to TDB-10-1, the two experiments share the same relative ratio of Q_w:Q_s. Finally, in the third experiment, TDB-11-1, Q_w was doubled relative to TDB-10-1, but Q_s and $\bar{r}$ were set equal to the control experiment, resulting in a Q_w:Q_s twice TDB-10-1.

[12] The sediment mixture used in all experiments was composed of 70% by volume quartz sand ($D_{50} = 110\ \mu m$) and 30% coal sand ($D_{50} = 440\ \mu m$). The coal has a specific gravity of 1.3, whereas quartz has a specific gravity of 2.65, so the coal grains are substantially more mobile than the quartz grains and serve as a proxy for fine-grained clastics. The mixture of quartz and coal is similar to that used in previous experiments [*Heller et al.*, 2001; *Sheets et al.*, 2007; *Martin et al.*, 2009]. In order to visualize the active channel network, the input water was dyed with a commercially available blue food coloring and made opaque by adding a small amount of titanium dioxide.

[13] Three types of data were collected from the experiments: system morphology, surface topography, and deposit stratigraphy. The morphologies of the fluvial systems were recorded with two digital cameras. One of the cameras was positioned to collect images of the entire basin, which were used to characterize surface dynamics, while the second camera was positioned to collect both surface morphology and topography data. Images of surface morphology were post-processed to remove camera distortion, resulting in images with horizontal resolution of approximately 0.7 pixels per mm. Both cameras recorded images of the active delta top at 1 min intervals. Topographic measurements were taken in a manner modeled on the Experimental Earthscape Facility (XES) subaerial laser topography scanner [*Sheets et al.*, 2007]. In contrast to XES, however, where the topography of the entire fluvial surface is recorded periodically, we chose to monitor topography at 2 min intervals along three flow-perpendicular transects, located 1.6 m, 2.1 m, and 2.6 m from the infeed point. This system uses oblique digital images of lines cast by vertical laser sheets from which true topography can be calculated. To measure a full cross-section of topography, including areas inundated by water, the experiment was stopped every 2 min, and water was allowed to drain off the fluvial surface prior to collecting measurements. This arrangement allows instantaneous (the exposure time of the camera) measurements rather than the 30 to 45 min required for a full-surface scan. With this system, we obtained measurements with horizontal and vertical resolution of ~1.0 mm. The three experiments each produced an average of 415 mm of stratigraphy. Following each experiment, we sectioned and imaged the deposits at each of the topographic strike-transects.

Table 1. Experimental Boundary Conditions

	Duration (h)	Q_s (L/s)	Q_w (L/s)	Q_w/Q_s (1/1)	Base-Level Rise Rate (mm/h)
TDB-10-1	78.2	0.011	0.451	41	5
TDB-10-2	39.3	0.022	0.902	41	10
TDB-11-1	77.2	0.011	0.902	82	5

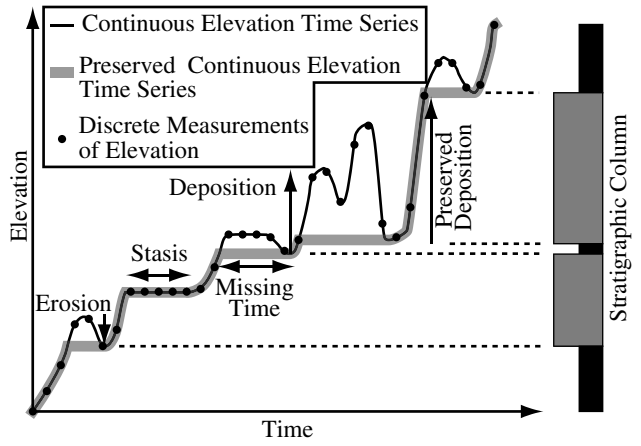

Figure 2. Schematic diagram illustrating the construction of a stratigraphic column from elevation increments and parameters controlling stratigraphic completeness. Preserved time in stratigraphy is housed in deposits constructed during positive elevation changes that are not later eroded. Gaps in the record occur as a result of stasis on the geomorphic surface and erosion.

3. Terminology

[14] We start by considering the lengthening of a stratigraphic column in 1-D. In Figure 2, we display a time-elevation curve for a horizontal point location in a generalized hypothetical basin. We recognize three categories of surface evolution on this curve: deposition, erosion, and stasis. Deposition is defined by periods with positive rates of elevation change, while erosion is defined as periods with negative rates of elevation change. We define stasis as periods with constant elevation. Definitions for deposition, erosion, and stasis as defined above are for basins with no subsidence and would thus need to be slightly altered to account for this term in settings with vertical surface motion not associated with sediment deposition or erosion. We note that our definition of stasis does not distinguish between periods associated with abandonment of a horizontal point location in a basin by a transport system and periods where active fluid flow occurs above that location with no elevation change (i.e., equilibrium topography).

[15] The resulting stratigraphy records portions of the depositional history not removed via periods of erosion [*Kolmogorov*, 1951; *Pelletier and Turcotte*, 1997; *Schumer et al*., 2011]. We recognize preserved deposition as periods associated with continuous deposition at a given measurement interval which have not been removed via later erosion and which are bounded above and below by erosional unconformities, paraconformities, or a mixture of the two [*Sadler and Strauss*, 1990]. Next, for a time series of elevations that are discretized with a defined time step, we define missing time within a record as stasis, erosion, or deposition later removed from the record by erosion. The stratigraphic column that results from such an erosional-depositional process can be generated from the elevation time series as shown in Figure 2. Stratigraphic deposits are depositional bodies bound between two preserved erosional boundaries [*Kolmogorov*, 1951; *Pelletier and Turcotte*, 1997; *Schumer et al*., 2011; *Straub et al*., 2012].

4. Compensation and Channel Time Scales

[16] In this section, we present theory for prediction of stratigraphic completeness as it relates to geomorphic processes. This theory is couched in two time scales influenced by Q_w and Q_s: a compensation time scale (T_c) and a channel time scale (T_{ch}), in addition to the time scale at which a record is discretized (t), which is set by the interpreter. The choice of these time scales allows for the characterization of three important components in the generation of stratigraphy: (1) the time-variant topography of an actively changing surface, (2) the kinematics by which the surface is changing and (3) the rate of net deposition.

[17] As illustrated in Figure 2, missing time in the stratigraphic record is a result of both erosion and stasis in net depositional settings. We start by characterizing the amount of time necessary for sediment deposited at a given time to be transferred into the stratigraphic record to a depth such that future episodes of erosion will be unable to remove it from the record. As each experiment in our study is associated with its own constant boundary conditions, we are only interested in erosion resulting from autogenic processes. This can be thought of as the time necessary to generate a deposit with a mean thickness equal to the maximum vertical roughness length scale of the transport system at any time. For delta environments, the maximum vertical roughness length scale can be approximated by the maximum depth of the system's channels [*Straub et al*., 2009]. This gives a compensation time scale, T_c, as developed by *Wang et al*. [2011] and used by *Ganti et al*. [2011] as follows:

$$T_c = \frac{H_c}{\bar{r}}, \tag{1}$$

where H_c is the maximum depth of channels for a given location in a basin and $\bar{r}$ is the basin-wide long-term sedimentation (or subsidence) rate.

[18] *Sadler and Strauss* [1990] demonstrate that stratigraphic completeness is strongly correlated to an interpreter's choice of t. We demonstrate this point below with our experiments and examine how stratigraphic completeness relates to a dimensionless time scale equal to the following:

$$\hat{t} = \frac{t}{T_C}. \tag{2}$$

[19] T_c as formulated above contains information pertaining to the time-variant topography of an actively changing surface (H_c) and the rate of net deposition ($\bar{r}$). Thus, we still need to characterize the kinematics by which a surface is changing. This is done using a time scale that inversely correlates with the lateral mobility of a system's channels, T_{ch}. *Cazanacli et al*. [2002] defined T_{ch} as the time necessary for channels to migrate over the entire width of a basin, thus visiting every point in a basin at least once. This time scale can be estimated using the following:

$$T_{\mathrm{ch}} = \frac{B_t - B_w}{v_c}, \tag{3}$$

where B_t is the total basin width, B_w is the total wetted width, and v_c is a characteristic rate of lateral channel movement (avulsion plus continuous migration). Further, *Paola et al*.

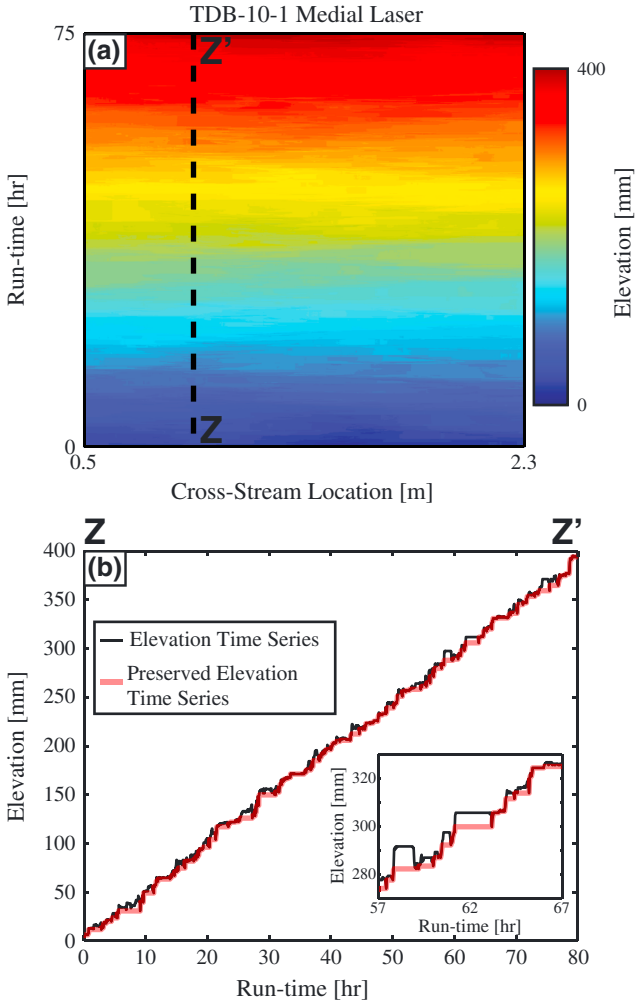

Figure 3. Data defining evolution of topography and surface dynamics for the medial laser location of the TDB-10-1 experiment. (a) Space-time-elevation map constructed from sequential delta top profiles shown every 2 min. (b) Example of time series of topography measured at a single location on the medial transect and resulting preserved record of elevation in the stratigraphy at this location.

[2001] and *Sheets* [2004] have shown that a velocity scale for channels can be calculated using a system's width averaged sediment discharge, q_s, and H_c:

$$v_c = \frac{q_s}{H_c}. \tag{4}$$

[20] In practice, *Kim et al.* [2010] showed that equations (3) and (4) well approximate the time necessary for 95% of a basin to be visited by flow in an experiment with no cross-stream subsidence gradient.

[21] Next, a time scale ratio can be formulated using T_c and T_{ch}:

$$T^* = \frac{T_c}{T_{ch}}. \tag{5}$$

[22] We hypothesize that for stratigraphic sections discretized by identical values of $\hat{t}$, T^* can be used to estimate stratigraphic completeness. It is important to note here that both T_c and T_{ch} are influenced by Q_w, Q_s, and base-level rise. As such, one cannot simply tune T_{ch} while keeping T_c constant, or vice versa, when aiming for a particular T^* value. However, T_c and T_{ch} do not scale with Q_w, Q_s, and base-level rise in exactly the same way; thus, a range of T^* is possible. One way to view T^* is as the minimum number of times channelized flow visits a site during the basin-wide aggradation of one H_c. This can be seen by comparing two deltas which share an equivalent T_c, but varying T_{ch}. Each spot on the delta characterized by the higher T_{ch} is infrequently visited by flow during a period of duration T_c and has a low T^*. Conversely, each spot on the delta characterized by the lower T_{ch} will be frequently visited by flow during the same period and have a higher T^*. We hypothesize that the latter scenario leads to frequent cut and fill episodes and thus low completeness, while the former scenario leads to deposits that are not often reworked and thus have high completeness.

[23] To explore parameters that set T^*, we expand equation (5) using equations (1), (3), and (4) resulting in the following:

$$T^* = \frac{H_c v_c}{\bar{r}(B_t - B_w)}. \tag{6}$$

[24] From equation (5), we note that systems characterized by high T^* include those with deep channels that laterally migrate fast and that systems characterized by low T^* include those with high aggradation rates. Here we hypothesize that systems with deep channels that laterally migrate fast in basins with low aggradation rates will have lower completeness than systems with shallow channels that migrate slowly in basins with high aggradation rates. This leads to the hypothesis that T^* is inversely correlated to stratigraphic completeness. Further, for the special case where a delta is undergoing pure aggradation with no average change in shoreline location, equation (6) reduces to the following:

$$T^* = \frac{A}{B_w(B_t - B_w)}, \tag{7}$$

where A is delta-top area. Thus, equation (7) suggests that in settings characterized by pure aggradation, in the absence of progradation, T^* can be estimated solely from knowledge of delta area, the width of a cross-section, and its wetted fraction.

5. Experimental Results

[25] In this section, we summarize statistics that characterize the surface morphology and dynamics of our three experiments and also provide a detailed statistical characterization of the constructed (synthetic) stratigraphy using the surface elevation time series. All 1-D statistics presented in this section were computed on the ensemble of time series along each topographic transect. Aggradation of each fan-delta resulted from the transport and deposition of sediment by migrating channelized flows (Figure 1). An example time-space-elevation map for one of the experiments is shown in Figure 3a. While the long-term elevation drift dominates this matrix, analysis of an elevation time series at any one cross-stream location reveals a record composed of periods of stasis, erosion, and deposition (Figure 3b), similar to the schematic elevation time series in Figure 2.

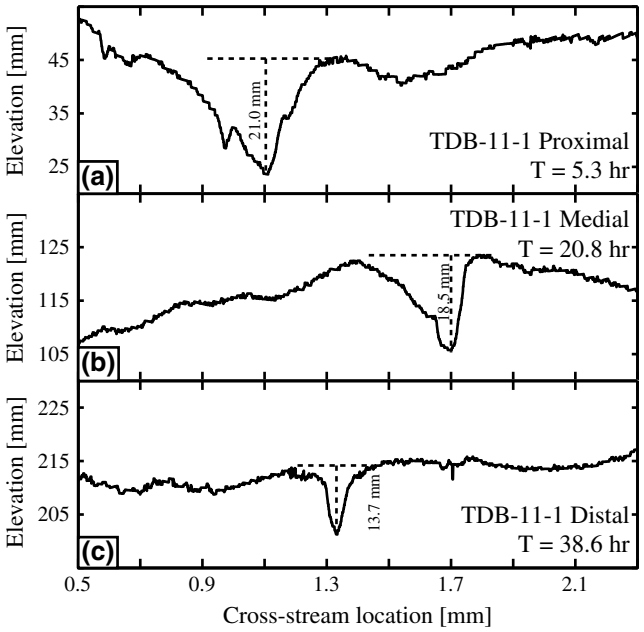

Figure 4. Proximal, medial, and distal elevation transects from TDB-11-1 with channel depth highlighted. Horizontal dashed lines represent approximate upper surface of channelized flow, and vertical dashed lines represent extent of channel depths.

5.1. Estimation of Compensation and Channel Time Scales

[26] The formulations for T_c and T_{ch} as defined in equations (1) and (2) each contain variables which cannot, at present, be predicted from boundary conditions with high precision. These variables include the maximum depth of channels (H_c) and the strike-oriented width of flow covering a basin (B_w). We use topographic measurements and overhead images of the active fluvial surfaces to quantify parameters that allow us to estimate T_c and T_{ch}.

[27] Utilizing coregistered topographic scans and images of the active transport system, we generate distributions of flow depth for each experiment at each transect location (Figure 4). As we are interested in maximum flow depth, we estimate H_c as the value corresponding to the 95th percentile on cumulative distribution plots of flow depth. In Figure 5a, we present measurements of H_c for each experiment at each transect. We choose to display H_c as a function of the dimensionless mass extraction parameter, χ, which represents the fraction of supplied sediment flux lost to deposition up to a position x [*Strong et al.*, 2005; *Paola and Martin*, 2012]. The flux lost to deposition is the integral of the net rate of deposition $\bar{r}$ over the distance x. Thus, for an initial total sediment flux Q_{so}, the value of χ at a given location is given by the total sediment flux lost to deposition normalized by Q_{so}, which can be determined as follows:

$$\chi(x) = \frac{1}{Q_{s0}} \int_0^x B_t(x')r(x')dx'. \quad (8)$$

For each of the experiments, a decrease in H_c is observed with increases in χ. In addition, at all values of χ, H_c for TDB-10-2 and TDB-11-1 are similar to each other and larger than TDB-10-1.

[28] Measurements of H_c coupled with values of $\bar{r}$ allow us to calculate T_c for all measurement transect locations using equation (1). For each experiment, we observe a decrease in T_c as a function of χ. At any value of χ, TDB-11-1 has the longest T_c, followed by TDB-10-1 and then TDB-10-2 (Figure 5b).

[29] Next, we tackle T_{ch}. First we directly measure it using our library of overhead photos, and then we use equations (3) and (4) to estimate T_{ch} for each transect in each experiment. Measuring T_{ch} is accomplished using wet/dry maps of experimental surfaces generated from overhead photos. Using a threshold blue luminosity value, we separate dry regions from wet regions on each delta-top image [*Tal et al.*, 2012]. The threshold value used for this operation was picked by identifying a value that on visual inspection appeared to correctly separate the two regions. We generate wet/dry maps for every 1 min of the three experiments. We then track dry fraction, f_d, reduction by monitoring the fraction of each measurement transect yet to be visited by flow for 5 h windows, starting every 0.5 h of run time. For each experiment, the resulting dry-fraction reduction curves are then ensemble averaged to produce one representative curve for each measurement transect. f_d reduction curves for the three experiments at the proximal measurement transect location are shown in Figure 6a. On these curves, the value of f_d at time zero, $f_{d,t=0}$, represents the average fraction of a transect not occupied by flow (or 1 minus the fraction inundated with flow) during an experiment at any instant in time. We note that $f_{d,t=0}$ is greatest for TDB-10-1 at ~0.64, while TDB-10-2 and TDB-11-1 are characterized by $f_{d,t=0}$ of 0.41 and 0.42, respectively. These measurements are consistent with the twofold increase of Q_w in TDB-10-2 and TDB-11-1 relative to TDB-10-11.

[30] Next, we estimate T_{ch} as $t(f_d = 5\%)$, the time necessary for flow to visit 95% of the transect. Previous studies have shown that $t(f_d = 5\%)$ compares favorably with equation (3) [*Kim et al.*, 2010]. For all transects, we observe increases in T_{ch} from TDB-10-2 to TDB-10-1 to TDB-11-1 (Figure 6b, Table 2). To isolate the influence of Q_w:Q_s on channel mobility, we normalize curves of f_d by their associated $f_{d,t=0}$ (Figure 6c). Following this normalization, we observe a similar decay of f_d with time in TDB-10-1 and TDB-10-2, which have equivalent ratios of Q_w:Q_s. A slower decay of f_d with time is observed in TDB-11-1, suggesting that increases in Q_w:Q_s reduce channel mobility, as has been seen in other experiments [*Cazanacli et al.*, 2002; *Powell et al.*, 2012].

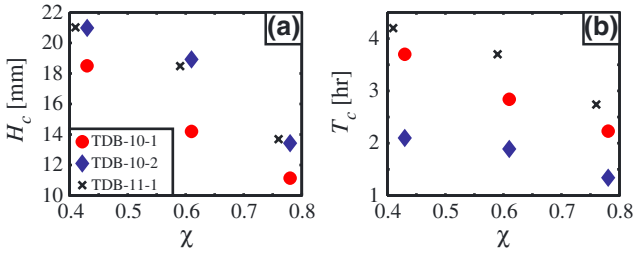

Figure 5. Data defining proximal to distal changes in (a) maximum channel depth and (b) compensation time scale at the three measurement locations for the three experiments (TDB-10-1: red circles; TDB-10-2: blue diamonds; TDB-11-1: black crosses) in the study.

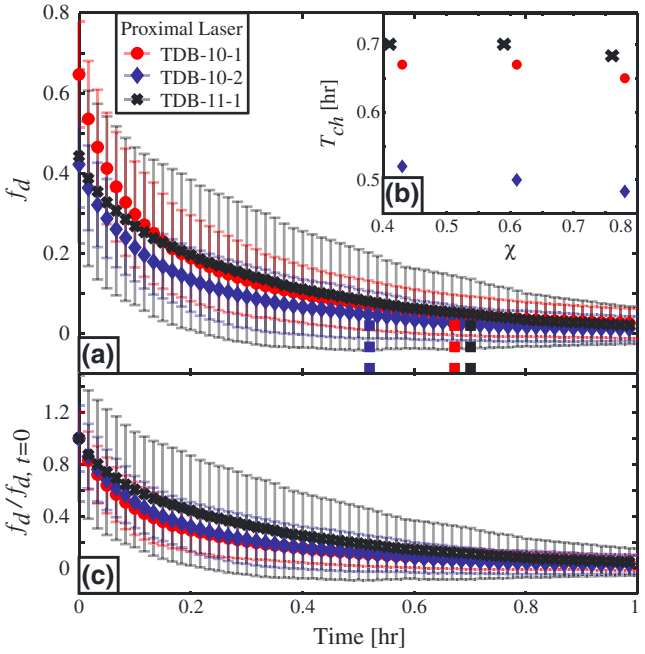

Figure 6. Data defining the reduction in remaining dry fraction on the fluvial surface as a function of time, used to estimate T_{ch}. (a) Mean dry-fraction reduction curves for the three experiments in the study. Thick dashed lines represent time associated with dry-fraction curve failing below 5% in each experiment. (b) Data defining proximal to distal changes in T_{ch} at the three measurement locations for the three experiments in the study. (c) Mean dry-fraction reduction curves presented in Figure 6a normalized by $f_{d,t=0}$. Error bars in all three panels represent geometric standard deviation of each measurement.

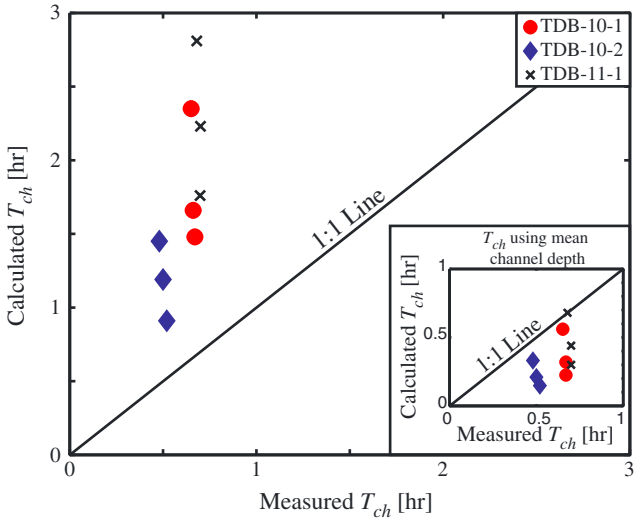

Figure 7. Comparison of measured and calculated values for T_{ch}. Calculated T_{ch} values in main plot use maximum channel depth for each transect in each experiment. Insert plot contains comparison of measured and calculated values of T_{ch} with mean channel depth used in calculation. Solid lines are lines of perfect agreement.

[31] With compiled data on channel depths and the average transect fraction occupied by flow, we now have the data necessary to calculate estimates of T_{ch} using equations (3) and (4) and compare these estimates to our measurements. We use our estimates of $f_{d,t=0}$, input Q_s, and χ to calculate B_w and q_s for each transect in each experiment. We find that the calculated estimates of T_{ch} are all larger than the measured T_{ch} values (Figure 7). This is likely a consequence of the use of maximum channel depths in formulating H_c over use of a mean channel depth. When using mean channel depths, our estimated T_{ch} values move closer to our measured T_{ch} values. Examination of our measured and estimated T_{ch} values reveal that both share the same trend in channel mobility between experiments with TDB-10-2 being the most mobile followed by TDB-10-1 and TDB-11-1, which share similar channel mobility. However, in any one experiment, equations (3) and (4) predict a decrease in channel mobility from source to sink, while our measurements reveal the opposite trend. We believe this is associated with nonlocal effects influencing T_{ch}. Equations (3) and (4) utilize local measurements of wetted width, q_s and H_c, but in addition to these local parameters, we hypothesize that mobility of channels upstream of a point of interest also influences channel mobility, particularly in sites with rapid gradients in wetted width, q_s, and H_c. We believe that the discrepancy between our estimated and measured T_{ch} values points to the need for further development of theory capable of predicting channel mobility. For the remainder of this manuscript, we utilize our measured values of T_{ch} in examining stratigraphic completeness.

5.2. Measuring Stratigraphic Completeness

[32] We start our analysis of stratigraphic completeness by measuring it at the finest temporal resolution available to us

Table 2. Internally Generated Experimental Parameters

	χ (1/1)	H_c (mm)	T_c (h)	Estimated T_{ch} (h)	Measured T_{ch} (h)	T^* (1/1)
TDB-10-1						
Proximal	0.43	18.5	3.70	1.48	0.67	5.52
Medial	0.61	14.2	2.84	1.66	0.67	4.24
Distal	0.78	11.1	2.23	2.35	0.65	3.43
TDB-10-2						
Proximal	0.43	21.0	2.10	0.91	0.52	4.03
Medial	0.61	18.9	1.89	1.19	0.50	3.78
Distal	0.78	13.4	1.34	1.45	0.48	2.78
TDB-11-1						
Proximal	0.41	21.0	4.20	1.76	0.70	6.01
Medial	0.59	18.5	3.70	2.23	0.70	5.29
Distal	0.76	13.7	2.74	2.81	0.68	4.01

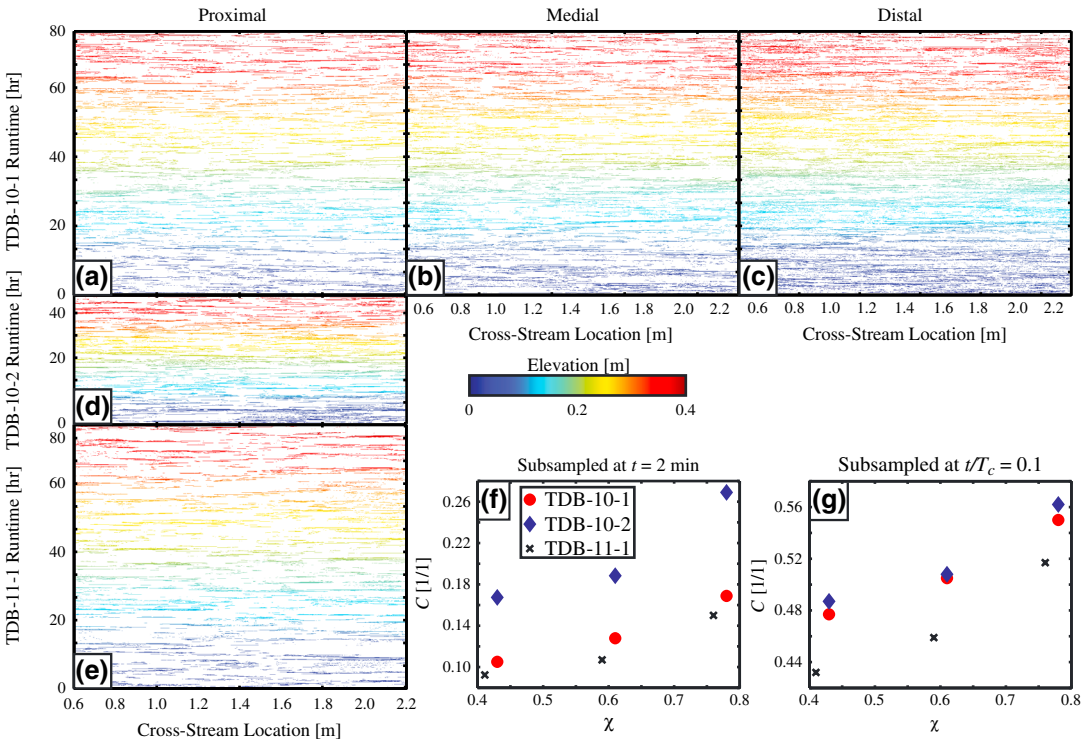

Figure 8. Time-space-elevation maps of preserved elevation (a, b, c) at the three measurement transects of TDB-10-1 and (a, d, e) at the proximal measurement transect for the three experiments with t equal to 2 min and (f, g) associated plots of C. White regions in maps represent time-space pairs where either stasis or erosion resulted in lack of preserved time by way of preserved deposits in the stratigraphic record.

in our three experiments, that being with t set to 2 min. We define stratigraphic completeness, C, as the fraction of time intervals, n, along a 1-D stratigraphic section discretized at t, which leaves a record in the form of preserved sediment over the length of a section that has a total time, T:

$$C = \frac{nt}{T}. \tag{9}$$

[33] In Figures 8a–8e, we present time-space-elevation maps of preserved deposition for measurement transects in the three experiments. From these maps, it is apparent that at this value of t, gaps in the preserved record are present over a range of time and length scales as predicted by theory of *Strauss and Sadler* [1989] and *Schumer and Jerolmack* [2009]. Using equation (9), we calculate C for all transects in the three experiments and find the following results: (1) For all experiments, C increases from proximal to distal in the basin, and (2) at a given value of χ, C is greatest for TDB-10-2 followed by TDB-10-1 then TDB-11-1 (Figure 8f).

[34] Motivated by the work of *Ager* [1973] and *Sadler and Strauss* [1990], our next step is to analyze the effect of t on C. For each data set, we first generate synthetic stratigraphy by stacking elevation time series and clipping the time series for elevations removed via erosion at the finest temporal resolution available [*Martin et al.*, 2009; *Wang et al.*, 2011]. We then proceed by systematically coarsening the temporal resolution of our synthetic stratigraphy from the initial measurement resolution to a final resolution equal to $0.5T$, for each experiment, by Δt steps of 2 min. Then for each value of t we apply equation (9) to calculate C. Sample time-space-elevation maps

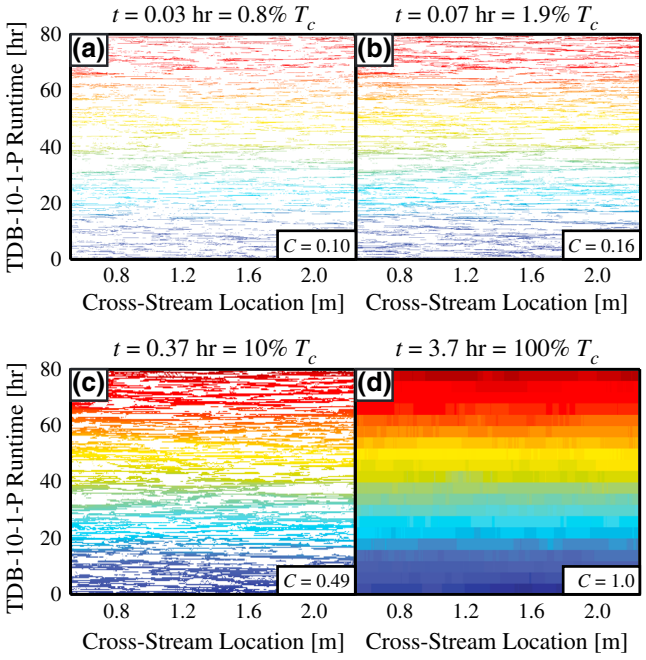

Figure 9. Time-space-elevation maps of preserved elevation of the proximal measurement transect of the TDB-10-1 experiment. Raw elevation time series are discretized at four values of t, and stratigraphic completeness is calculated for each new data set. White regions in maps represent time-space pairs where either stasis or erosion resulted in lack of preserved time by way of preserved deposits in the stratigraphic record.

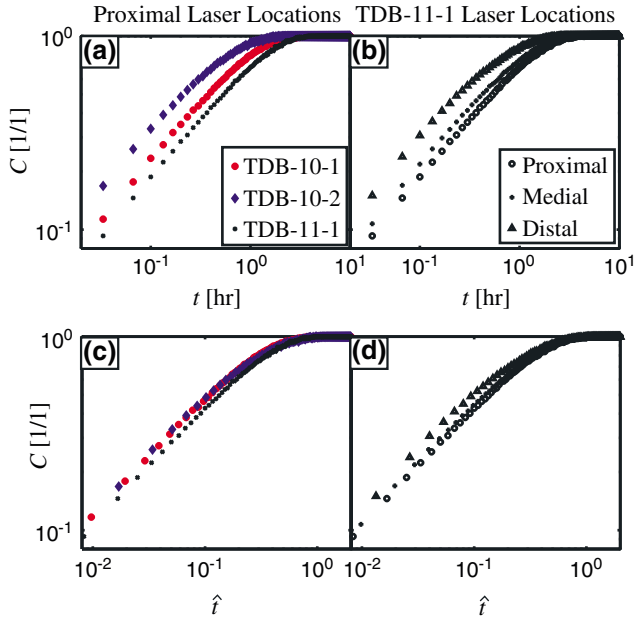

Figure 10. Stratigraphic completeness versus time scale of discretization in both (a, b) dimensional and (c, d) dimensionless space for the proximal measurement transect for the three experiments (in Figures 10a and 10c) and at the three measurement transects of TDB-10-1 (in Figures 10b and 10d).

of preserved deposits for four values of t at the proximal transect of TDB-10-1 are shown in Figure 9. From these maps, we observe an increase in C with increasing t as predicted by *Sadler and Strauss* [1990]. A full analysis of the dependency of C over the full range of t values available to us results in the following observations: (1) At each measurement transect, C appears to increase as a power-law function of t (observed as a linear increase of C versus t in log-log plots) for a range of t values until a rollover in the trend occurs as C approaches 1 (Figure 10); (2) for a given value of χ, TDB-10-2 has the highest C, followed by TDB-10-1 and TDB-11-1 at all values of t (Figure 10a); and (3) for a given experiment, C increases from proximal to distal in the basin for all values of t (Figure 10b).

[35] *Sadler and Strauss* [1990] examined C as a function of a dimensionless age by normalizing t by the total age of a section. This made sense in their study as their stochastic sedimentation models were built from elevation increment distributions which lacked truncation by physical processes. As a result, erosional events with exceptionally large magnitude occasionally occurred. In many systems, physical constraints place upper and lower limits on distributions [*Zhang et al.*, 2007; *Ganti et al.*, 2011]; for example, in our experiments the maximum size of erosional events is set by H_c, and as a result we choose to normalize t by T_c. This operation brings curves of C from all measurement transects in all experiments into close agreement (Figures 10c and 10d). For all curves, we observe a power-law increase in C between $\hat{t}$ values of 0.01 and 0.1, described by the following:

$$C = a\hat{t}^{\alpha}, \tag{10}$$

where a is a leading coefficient and α is an exponent describing the growth of the power law. Between $\hat{t}$ values of 0.01 and 0.1, the C curves in this study are described by α values between 0.54 and 0.70. A rollover in the trend of C is then observed between $\hat{t}$ values of 0.1 and 1 with C saturating at 1 for values equal to or greater than 1. While our formulation for dimensionless time brings curves of C into close agreement, the collapse is not perfect. At any one transect, we observe that C for TDB-11-1 is less than the other two experiments for all values of $\hat{t}$ (Figure 10c). In addition, for any one experiment, C increases from proximal to distal locations (Figure 10d).

[36] Next, we analyze how C varies as a function of T^*. This is done as the normalization of t by T_c described above brings curves of C into close but not complete agreement. In their stochastic models, *Sadler and Strauss* [1990] found that comparing models of equivalent dimensionless age did not bring completion curves from all models into agreement. To bring models into agreement, Sadler and Strauss show that they must share similar dimensionless ages and a term they defined as dimensional drift, which is a parameter that normalizes the long-term sediment accumulation rate by the variability in that rate. Here we use T^* as a method to nondimensionalize a parameter, channel mobility, that is correlated with variability in deposition rates. Utilizing measurements of T_c and T_{ch}, we calculate T^* for the three experiments at the three measurement transects, which results in a range of T^* values for the nine data sets between 2.5 and 6.0. Earlier in this manuscript, we hypothesized that the higher an environment's T^* the more prone it is to cut and fill events that lower completeness during the basin-wide aggradation of a deposit with thickness equal to H_c. In Figure 11, we compare time series of topography from a low T^* setting (distal transect of TDB-10-2) with a high T^* setting (proximal transect of TDB-11-1). The time series have equivalent duration when normalized by T_{ch}, and for comparison purposes, we normalize elevations by the H_c characterizing each transect. Similar to our hypothesis, we observe that the elevation time series for the high T^* setting is

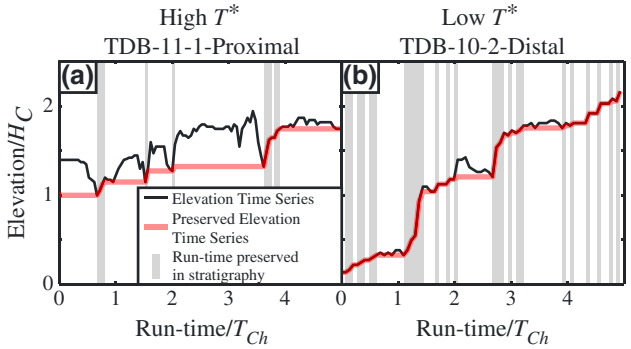

Figure 11. Data defining evolution of topography and completeness of preserved stratigraphic record for (a) high and (b) low T^* environments. Time series of topography measured at the center of the proximal transect of the TDB-11-1 experiment (in Figure 11a). Time series of topography measured at the center of the distal transect of the TDB-10-2 experiment (in Figure 11b). Time series begin exactly halfway through each respective experiment and share equivalent duration when normalized by T_{ch}. Elevations in both time series are normalized by the H_c value characterizing each data set.

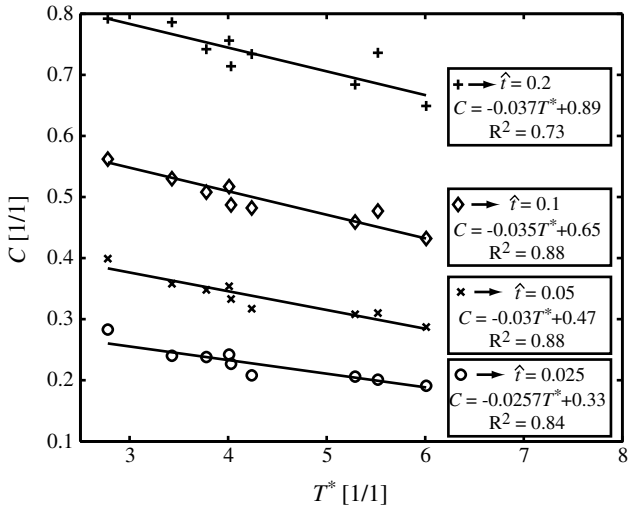

Figure 12. Measured stratigraphic completeness versus T^* for all transects from three experiments where elevation time series were discretized by four values of $\hat{t}$. Solid lines represent best fit linear regressions for data sets sharing same $\hat{t}$ of discretization.

characterized by frequent cut and fill events and low stratigraphic completeness when compared to the low T^* setting.

[37] To more fully examine the dependence of C on T^*, we generate a plot that incorporates the three transects from the three experiments. When plotting C as a function of T^*, one needs to choose a time scale to discretize an elevation time series. We choose to discretize each elevation data set by four predefined values of dimensionless time, $\hat{t}$, equal to 0.025, 0.05, 0.1, and 0.2, thus producing four data sets in which we can plot C versus T^* (Figure 12). Over the range of T^* values provided us by our experiments, we find that C is inversely correlated with T^*, for example decreasing from 0.28 to 0.19 as T^* increases from 2.5 to 6.0, when discretized with $\hat{t}$ equal to 0.025.

6. Discussion

6.1. Influence of Q_w and Q_s on Stratigraphic Completeness

[38] The relationship between Q_w and Q_s to stratigraphic completeness, as detailed above, depends on the question one poses. From our perspective, we see two first-order types of records one might be interested in extracting from stratigraphy. The first pertains to using the stratigraphic record to answer questions that are unrelated to the interworkings of the sediment transport system, for example a chemical signal useful as a regional or global climate proxy that is fixed to deposited sediment [*Fike et al*., 2006; *Maloof et al*., 2010]. The second pertains to using the stratigraphic record to extract information regarding the processes and products of a sediment transport system [*Mohrig et al*., 2000; *Jerolmack and Sadler*, 2007; *Shen et al*., 2012]. Our experimental results suggest that the magnitudes of Q_w and Q_s impact these two types of records in different ways.

[39] We start by analyzing the influence of Q_w and Q_s on stratigraphic completeness as it pertains to extracting proxy signals affixed to deposited sediment which are disconnected from the sediment routing system. For these records, it is most useful to have the greatest resolution possible in dimensional time, t. For this, one wants a system with short T_c, as completeness scales with $\hat{t}$. The experiment with the shortest T_c in our study was TDB-10-2 (Figure 5b). This is consistent with the experimental results where we find that TDB-10-2 has the highest stratigraphic completeness for any choice of t (Figures 10a and 10b). In this experiment, the high input Q_s and Q_w resulted in the most mobile transport system of the study and also a system with deep channels relative to the other two experiments, both of which work against completeness. These correlations are consistent with theory for prediction of system mobility and channel depth as functions of Q_w and Q_s [*Sheets*, 2004; *Powell et al*., 2012]. However, $\bar{r}$ of TDB-10-2 was twice that of the other two experiments, which works for stratigraphic completeness. A comparison of channel mobility, H_c, and $\bar{r}$, though, reveals that the magnitude of the changes in $\bar{r}$ exceeds the other parameters. As a result, TDB-10-2 has the lowest T_c of the three experiments and thus the greatest C.

[40] For stratigraphic studies that aim to extract high resolution information regarding sequencing of events associated with a morphodynamic process, it is generally helpful to nondimensionalize parameters important to system evolution [*Jerolmack and Mohrig*, 2007; *Kim et al*., 2010]. This is also true for our study. For example, suppose one is interested in using the stratigraphic record to examine morphodynamic processes that are scale independent, e.g., avulsion, channel mobility, etc. It might be helpful to compare the construction of stratigraphic packages that share similar thicknesses when normalized by the depths of the channels that constructed the two packages. To do this, it would be helpful to have stratigraphy sampled at the same $\hat{t}$ for both basins. When this normalization is done with our experiments, we find that TDB-10-1 and TDB-10-2 share similar stratigraphic completeness, that is in excess to TBD-11-1 (Figures 8g and 10c) for any choice of $\hat{t}$. The magnitude in the difference of C between TDB-10-1 and TDB-10-2 compared to TDB-11-1 might seem small in our results (Figure 10c), but we emphasize that we varied Q_w:Q_s by only a factor of 2 in our experiments, while in natural systems this parameter can vary by several orders of magnitude [*Paola et al*., 1992]. Thus, it appears that stratigraphic completeness for systems discretized by the same $\hat{t}$ are influenced more by the ratio of Q_w to Q_s than by their absolute magnitudes. As a result, we expect small systems and large systems, which share the same Q_w:Q_s to fill space and store information in a similar fashion, just at different absolute scales. However, increasing Q_w:Q_s appears to lower stratigraphic completeness. Thus, alluvial fans, constructed at the terminus of bedrock canyons with low Q_w:Q_s, might have higher stratigraphic completeness of process information compared to large deltas constructed in regions with high Q_w:Q_s.

6.2. Influence of T^* on Stratigraphic Completeness

[41] In section 4, we hypothesized a relationship where C was inversely correlated with T^*. Data from our experiments provide a first glimpse into this relationship as they only span T^* values between 2.5 and 6.0 but support the hypothesized reduction in C with increasing T^*. Further analysis of these data reveal that at all transect locations, experiment TDB-11-1, which has the highest Q_w:Q_s, also has the highest T^* of the three

experiments (Table 2). What physical processes associated with changes in Q_w:Q_s cause the reduction in C for systems discretized with similar values of $\hat{t}$? Comparing TDB-11-1 to TDB-10-1, experiments with the same aggradation rate but which vary in Q_w:Q_s by a factor of 2, we find that channel mobility is roughly equal in both experiments (Figure 6). However, channels are significantly deeper in TDB-11-1 (Q_w:Q_s = 82) compared to those in TDB-10-1 (Q_w:Q_s = 41). So, while the two experiments share similar channel mobility, the increase in H_c results in reworking of sediment to greater depths in TDB-11-1 during one period of duration T_{ch} and thus lower C. The difference in H_c for these two experiments results in an increase in T_c from TDB-10-1 to TDB-11-1, which then drives the differences in the observed T^* values.

[42] A question one might pose is the following: Where on the C versus T^* domain do natural systems reside? While we do not have an exhaustive database to answer this question at present, we find it informative to look at one system, the Mississippi Delta. Using measurements of H_c for the Mississippi delta and average long-term subsidence rates measured for the last 8 Myr from biostratigraphic dates [*Straub et al*., 2009], *Wang et al*. [2011] calculated a T_c for the Mississippi Delta of 115 kyr. We make an order of magnitude estimate for T_{ch} using the amount of time associated with construction of the subdelta lobes that currently compose the Mississippi Delta-top plain. Using radiocarbon dating, *Tornqvist et al*. [1996] estimated ~7.5 kyr for this construction. Combining Wang et al. and Törnqvist et al. time scales yields an estimate of T^* for this region of ~15 or in a portion of the C versus T^* domain likely to have lower stratigraphic completeness than our experiments. This estimate is consistent with our experimental results as Q_w:Q_s for the Mississippi River is larger than that of any of our experiments [*Nittrouer et al*., 2011], and we find on average an increase in T^* with Q_w:Q_s.

6.3. Comparison to Previous Studies

[43] At this stage, we find it helpful to compare our findings on how stratigraphic completeness depends on t, T_c, and T_{ch} to findings in previous studies, specifically the theory and models of *Strauss and Sadler* [1989] and *Sadler and Strauss* [1990]. For the sake of this comparison, we focus on the stochastic models of sedimentation presented in these two manuscripts. This choice is made as these models more closely resemble our autogenic experiments than the deterministic models with cyclic boundary conditions discussed in *Sadler and Strauss* [1990]. These studies cast C as a function of two dimensionless numbers: dimensionless age, A^*, and dimensionless drift, D^*. Dimensionless age was defined as follows:

$$A^* = \frac{T_S}{t}, \tag{11}$$

where T_s is the total age of a stratigraphic column. Sadler and Strauss illustrated that given a mean background deposition rate and known unsteadiness of that rate, C initially decreases as A^* increases until approaching an asymptotic lower limit. This lower limit is set by a dimensionless drift, D^*, defined as follows:

$$D^* = \frac{\bar{r}}{\sigma}\sqrt{t}, \tag{12}$$

where σ is the standard deviation of the model elevation increments.

[44] In our analysis, $\hat{t}$ can be viewed as having a similar control on C as A^*. However, for the autogenic experiments discussed here, $\hat{t}$ gives an exact prediction for the time scale of discretization necessary for generation of a record with C equal to 1. This is due to the upper limit imposed on erosional events by the size of channels in each of our experiments. In the work of *Strauss and Sadler* [1989] and *Sadler and Strauss* [1990], no theoretical upper limit on erosional event size exists for the distribution of elevation increments generated from their Brownian motion models.

[45] Further, over the parameter space explored in our experiments, T^* has a similar, though inverse, influence on C as D^*. In our formulation, increasing T^* increases the unsteadiness in deposition rate relative to the long-term average drift. For example, consider a strike-transect of a system with T^* equal to 2. In this system, every spot on the strike transect will be visited by flow, at minimum, 2 times during a period of duration T_c. In contrast, a system characterized by T^* of 4 is visited by flow at least 4 times during a single T_c. Increasing the number of times a location is visited by flow during a single T_c will drive more cut and fill sequences during the aggradation of a deposit with thickness of H_c and thus increase the variability in deposition rate for deltaic settings.

[46] We view the framework proposed above, which cast C as a function of $\hat{t}$ and T^*, as a first step towards defining process based controls on stratigraphic completeness, which builds on and is complementary to the existing statistical framework. For systems with steady boundary conditions, our analysis allows for prediction of C. Much future work, though, remains. The power of the statistical analysis proposed by *Strauss and Sadler* [1989] and *Sadler and Strauss* [1990] lies in the ability to cast unsteadiness associated with both autogenic processes and allogenic forcings into a single probability distribution. While many recent studies highlight the strong control of autogenic processes on the organization of stratigraphy [*Kim and Paola*, 2007; *Straub et al*., 2009; *Hajek et al*., 2010], it remains true that allogenic forcings over a range of time and space scales also strongly influence the morphodynamics and stratigraphy of deltaic systems [*Van Wagoner*, 1995; *Sun et al*., 2002; *Martin et al*., 2009]. Further, while not discussed here, *Sadler and Strauss* [1990] also examined the influence of cyclic forcings on C, which have long been theorized to exert strong control on sediment routing systems [*Sloss*, 1963; *Vail et al*., 1977; *Perlmutter et al*., 1998]. These stochastic and cyclic allogenic forcings likely influence T_c and T_{ch} of natural systems and thus need to be explored to formulate a more universal process framework for prediction of stratigraphic completeness.

7. Summary

[47] Motivated by previous studies that examine the completeness of the stratigraphic record with global compilations of deposition rates and stochastic models [*Strauss and Sadler*, 1989; *Sadler and Strauss*, 1990], this paper presents a framework for analysis of stratigraphic completeness as a function of time scales set by system boundary conditions. The main results are summarized as follows:

[48] 1. We develop a framework for quantifying stratigraphic completeness which uses two time scales that when combined quantify aspects of the time-variant topography of

sediment transport systems, the kinematics by which the topography changes, and the rate of net deposition to quantify stratigraphic completeness. The first of these time scales, T_c, quantifies the amount of time necessary to generate a deposit with a mean thickness equal to the maximum vertical roughness length scale over the area of a delta top. The second time scale, T_{ch}, characterizes the mobility of channels on delta tops.

[49] 2. Stratigraphic completeness increases as a function of the time scale at which a record is discretized, t, for all stratigraphic sections analyzed. When plotted as a function of dimensional time, the system with the shortest T_c had the greatest stratigraphic completeness. This corresponded to the experiment with the greatest Q_w and Q_s and $\bar{r}$. When normalizing t by T_c, we find that stratigraphic completeness increases as the ratio of Q_w to Q_s decreases. These two results suggest that preservation of environmental signals disconnected from a sediment routing system are best preserved in systems with high water and sediment fluxes coupled to rapid aggradation, while preservation of information characterizing system morphodynamics is best preserved in deltaic stratigraphy constructed by systems with low Q_w-to-Q_s ratios.

[50] 3. Over the parameter space analyzed, stratigraphic completeness decreases as the ratio of T_c to T_{ch} increases for systems discretized with the same value of $\hat{t}$. This result suggests that stratigraphic completeness in deltaic settings is controlled by the balance of system aggradation to lateral channel migration. In this framework, rapid aggradation relative to lateral channel migration favors high stratigraphic completeness, while rapid lateral migration of deep channels relative to system aggradation results in frequent deposit reworking. Order of magnitude calculation of this parameter for the Mississippi Delta suggests that stratigraphic completeness in many natural systems is even lower than measured in our experiments.

[48] **Acknowledgments.** We thank J. Kuykendall, whose expertise made the experiments described in this work possible; Y. Wang, Q. Li, K. Pennuto, and A. Breaux for help conducting the experiments discussed in the text; B. Sheets, C. Paola, R. Schumer, and V. Ganti for stimulating discussions that motivated and clarified several ideas in this manuscript. The editorial staff of *JGR-Earth Surface*, David Hoyal, and an anonymous reviewer are thanked for constructive reviews. We gratefully acknowledge support by National Science Foundation grant OCE-1049387 to Straub.

References

Abels, H. A., H. A. Aziz, W. Krijgsman, S. J. B. Smeets, and F. J. Hilgen (2010), Long-period eccentricity control on sedimentary sequences in the continental Madrid Basin (middle Miocene, Spain), *Earth Planet. Sci. Lett.*, *289*(1–2), 220–231, doi:10.1016/j.epsl.2009.11.011.

Ager, D. V. (1973), *The Nature of the Stratigraphic Record*, 114 pp., Wiley, New York.

Allen, P. A., and J. R. Allen (1990), *Basin Analysis: Principles and Applications*, 451 pp., Blackwell Scientific Publications, Oxford.

Aslan, A., W. J. Autin, and M. D. Blum (2005), Causes of river avulsion: Insights from the Late Holocene avulusion history of the Mississippi River, U.S.A., *J. Sediment. Res.*, *75*, 650–664.

Aziz, H. A., A. Di Stefano, L. M. Foresi, F. J. Hilgen, S. M. Laccarino, K. F. Kuiper, F. Lirer, G. Salvatorini, and E. Turco (2008a), Integrated stratigraphy and (40)Ar/(39)Ar chronology of early Middle Miocene sediments from DSDP Leg 42A, Site 372 (Western Mediterranean), *Palaeogeogr. Palaeoclimatol. Palaeoecol.*, *257*(1–2), 123–138, doi:10.1016/j.palaeo.2007.09.013.

Aziz, H. A., F. J. Hilgen, G. M. van Luijk, A. Sluijs, M. J. Kraus, J. M. Pares, and P. D. Gingerich (2008b), Astronomical climate control on paleosol stacking patterns in the upper Paleocene-lower Eocene Willwood Formation, Bighorn Basin, Wyoming, *Geology*, *36*(7), 531–534, doi:10.1130/G24734a.1.

Blum, M. D., and A. Aslan (2006), Signatures of climate vs. sea-level change within incised valley-fill successions: Quaternary examples from the Texas Gulf Coast, *Sediment. Geol.*, *190*(1–4), 177–211.

Catuneanu, O., A. J. Willis, and A. D. Miall (1998), Temporal significance of sequence boundaries, *Sediment. Geol.*, *121*(3–4), 157–178.

Cazanacli, D., C. Paola, and G. Parker (2002), Experimental steep, braided flow: Application to flooding risk on fans, *J. Hydraul. Eng.*, *128*, 322–330.

Clarke, L., T. A. Quine, and A. Nicholas (2010), An experimental investigation of autogenic behaviour during alluvial fan evolution, *Geomorphology*, *115* (3–4), 278–285, doi:10.1016/j.geomorph.2009.06.033.

Edmonds, D. A., D. C. J. D. Hoyal, B. A. Sheets, and R. L. Slingerland (2009), Predicting delta avulsions: Implications for coastal wetland restoration, *Geology*, *37*(8), 759–762, doi:10.1130/G25743a.1.

Fike, D. A., J. P. Grotzinger, L. M. Pratt, and R. E. Summons (2006), Oxidation of the Ediacaran Ocean, *Nature*, *444*(7120), 744–747, doi:10.1038/Nature05345.

Ganti, V., K. M. Straub, E. Foufoula-Georgiou, and C. Paola (2011), Space-time dynamics of depositional systems: Experimental evidence and theoretical modeling of heavy-tailed statistics, *J. Geophys. Res.*, *116*, F02011, doi:10.1029/2010JF001893.

Gardner, T. W., D. W. Jorgensen, C. Shuan, and C. R. Lemieux (1987), Geomorphic and tectonic process rates: Effects of measured time interval, *Geology*, *15*, 259–261.

Hajek, E. A., P. L. Heller, and B. A. Sheets (2010), Significance of channel-belt clustering in alluvial basins, *Geology*, *38*(6), 535–538.

Heller, P. L., C. Paola, I. Hwang, B. John, and R. Steel (2001), Geomorphology and sequence stratigraphy due to slow and rapid base-level changes in an experimental subsiding basin (XES 96-1), *AAPG Bull.*, *85*(5), 817–838.

Hickson, T. A., B. A. Sheets, C. Paola, and M. Kelberer (2005), Experimental test of tectonic controls on three-dimensional alluvial facies architecture, *J. Sediment. Res.*, *75*(4), 710–722.

Hinnov, L. A. (2000), New perspectives on orbitally forced stratigraphy, *Annu. Rev. Earth Planet. Sci.*, *28*, 419–475.

Holbrook, J. (2001), Origin, genetic interrelationships, and stratigraphy over the continuum of fluvial channel-form bounding surfaces: An illustration from middle Cretaceous strata, southeastern Colorado, *Sediment. Geol.*, *144*(3–4), 179–222.

Hoyal, D. C. J. D., and B. A. Sheets (2009), Morphodynamic evolution of experimental cohesive deltas, *J. Geophys. Res.*, *114*, F02009, doi:10.1029/2007JF000882.

Jerolmack, D. J., and D. Mohrig (2007), Conditions for branching in depositional rivers, *Geology*, *35*(5), 463–466, doi:10.1130/G23308a.1.

Jerolmack, D. J., and C. Paola (2007), Complexity in a cellular model of river avulsion, *Geomorphology*, *91*, 259–270.

Jerolmack, D. J., and C. Paola (2010), Shredding of environmental signals by sediment transport, *Geophys. Res. Lett.*, *37*, L19401, doi:10.1029/2010GL044638.

Jerolmack, D. J., and P. Sadler (2007), Transience and persistence in the depositional record of continental margins, *J. Geophys. Res.*, *112*, F03S13, doi:10.1029/2006JF000555.

Kim, W., and C. Paola (2007), Long-period cyclic sedimentation with constant tectonic forcing in an experimental relay ramp, *Geology*, *35*(4), 331–334, doi:10.1130/G23194a.1.

Kim, W., C. Paola, J. B. Swenson, and V. R. Voller (2006), Shoreline response to autogenic processes of sediment storage and release in the fluvial system, *J. Geophys. Res.*, *111*, F04013, doi:10.1029/2006JF000470.

Kim, W., B. Sheets, and C. Paola (2010), Steering of experimental channels by lateral basin tilting, *Basin Res.*, *22*(3), 286–301, doi:10.1111/j.1365-2117.2009.00419.X.

Kolmogorov, A. N. (1951), *Solution of a Problem in Probability Theory Connected with the Problem of the Mechanism of Stratification*, 8 pp., American Mathematical Society, New York.

Maloof, A. C., J. Ramezani, S. A. Bowring, D. A. Fike, S. M. Porter, and M. Mazouad (2010), Constraints on early Cambrian carbon cycling from the duration of the Nemakit-Daldynian-Tommotian boundary delta C-13 shift, Morocco, *Geology*, *38*(7), 623–626, doi:10.1130/G30726.1.

Martin, J., C. Paola, V. Abreu, J. Neal, and B. Sheets (2009), Sequence stratigraphy of experimental strata under known conditions of differential subsidence and variable base level, *AAPG Bull.*, *93*(4), 503–533.

Meyers, S. R. (2012), Seeing red in cyclic stratigraphy: Spectral noise estimation for astrochronology, *Paleoceanography*, *27*, doi:10.1029/2012PA002307.

Mohrig, D., P. L. Heller, C. Paola, and W. J. Lyons (2000), Interpreting avulsion process from ancient alluvial sequences: Guadalope-Matarranya (northern Spain) and Wasatch Formation (western Colorado), *GSA Bull.*, *112*, 1787–1803.

Nittrouer, J. A., D. Mohrig, and M. Allison (2011), Punctuated sand transport in the lowermost Mississippi River, *J. Geophys. Res.*, *116*, F04025, doi:10.1029/2011JF002026.

Paola, C. (2000), Quantitative models of sedimentary basin filling, *Sedimentology*, *47*, 121–178.

Paola, C., P. L. Heller, and C. L. Angevine (1992), The large-scale dynamics of grain-size variation in alluvial basins, 1: Theory, *Basin Res.*, *4*, 73–90.

Paola, C., and J. M. Martin (2012), Mass-balance effects in depositional systems, *J. Sediment. Res.*, *82*(5–6), 435–450, doi:10.2110/Jsr.2012.38.

Paola, C., et al. (2001), Experimental Stratigraphy, *GSA Today*, 4–9.

Paola, C., K. M. Straub, D. Mohrig, and L. Reinhardt (2009), The "unreasonable effectiveness" of stratigraphic and geomorphic experiments, *Earth-Sci. Rev.*, *97*, 1–43.

Pelletier, J. D., and D. L. Turcotte (1997), Sythetic stratigraphy with a stochastic diffusion model of fluvial sedimentation, *J. Sediment. Res.*, *67*, 1060–1067.

Perlmutter, M. A., B. J. Radovich, M. D. Matthews, and C. G. S. C. Kendall (1998), The impact of high-frequency sedimentation cycles on stratigraphic interpretation, in *Sequence Stratigraphy—Concepts and Applications. Special Publication of the Norwegian Petroleum Society*, edited by F. M. Grandstein, K. O. Sandvik, and N. J. Milton, pp. 141–170, Elsevier, Amsterdam.

Powell, E. J., W. Kim, and T. Muto (2012), Varying discharge controls on timescales of autogenic storage and release processes in fluvio-deltaic environments: Tank experiments, *J. Geophys. Res.*, *117*, F02011, doi:10.1029/2011JF002097.

Reitz, M. D., D. J. Jerolmack, and J. B. Swenson (2010), Flooding and flow path selection on alluvial fans and deltas, *Geophys. Res. Lett.*, *37*, L06401, doi:10.1029/2009GL041985.

Sadler, P. M. (1981), Sediment accumulation rates and the completeness of stratigraphic sections, *J. Geol.*, *89*, 569–584.

Sadler, P. M., and D. J. Strauss (1990), Estimation of completeness of stratigraphical sections using empirical data and theoretical-models, *J. Geol. Soc. London*, *147*, 471–485.

Schumer, R., and D. J. Jerolmack (2009), Real and apparent changes in sediment deposition rates through time, *J. Geophys. Res.*, *114*, F00a06, doi:10.1029/2009JF001266.

Schumer, R., D. J. Jerolmack, and B. McElroy (2011), The stratigraphic filter and bias in measurement of geologic rates, *Geophys. Res. Lett.*, *38*, L11405, doi:10.1029/2011GL047118.

Sheets, B. (2004), *Assembling the Alluvial Stratigraphic Record: Spatial and Temporal Sedimentation Patterns in Experimental Alluvial Systems*, 108 pp., University of Minnesota, Minneapolis, MN.

Sheets, B. A., T. A. Hickson, and C. Paola (2002), Assembling the stratigraphic record: Depositional patterns and time-scales in an experimental alluvial basin, *Basin Res.*, *14*, 287–301.

Sheets, B. A., C. Paola, and J. M. Kelberer (2007), Creation and preservation of channel-form sand bodies in an experimental alluvial system, in *Sedimentary Processes, Environments and Basins*, edited by G. Nichols, E. Williams, and C. Paola, pp. 555–567, Blackwell Publishing, Oxford, U.K.

Shen, Z., T. E. Tornqvist, W. J. Autin, Z. R. P. Mateo, K. M. Straub, and B. Mauz (2012), Rapid and widespread response of the Lower Mississippi River to eustatic forcing during the last glacial-interglacial cycle, *Geol. Soc. Am. Bull.*, *124*(5/6), 690–704.

Sloss, L. L. (1963), Sequences in the cratonic interior of North America, *Geol. Soc. Am. Bull.*, *74*, 93–114.

Straub, K. M., V. Ganti, C. Paola, and E. Foufoula-Georgiou (2012), Prevalence of exponential bed thickness distributions in the stratigraphic record: Experiments and theory, *J. Geophys. Res.*, *117*, F02003, doi:10.1029/2011JF002034.

Straub, K. M., C. Paola, D. Mohrig, M. A. Wolinsky, and T. George (2009), Compensational stacking of channelized sedimentary deposits, *J. Sediment. Res.*, *79*(9), 673–688.

Strauss, D., and P. M. Sadler (1989), Stochastic-models for the completeness of stratigraphic sections, *Math. Geol.*, *21*(1), 37–59.

Strong, N., and C. Paola (2008), Valleys that never were: Time surfaces versus stratigraphic surfaces, *J. Sediment. Res.*, *78*(7–8), 579–593.

Strong, N., B. A. Sheets, T. A. Hickson, and C. Paola (2005), A mass-balance framework for quantifying downstream changes in fluvial architecture, in *Fluvial Sedimentology VII, International Association of Sedimentologist, Special Publication 35*, edited by M. Blum, S. Marriott, and S. Leclair, pp. 243–253, Wiley-Blackwell, Oxford, U.K.

Sun, T., C. Paola, G. Parker, and P. Meakin (2002), Fluvial fan deltas: Linking channel processes with large-scale morphodynamics, *Water Resour. Res.*, *38*(8), 1151, doi:10.1029/2001WR000284.

Tal, M., P. Frey, W. Kim, E. Lajeunesse, A. Limare, and F. Metivier (2012), The use of imagery in laboratory experiments, in *Fluvial Remote Sensing for Science and Management*, edited by P. Carbonneau and H. Piegay, pp. 299–321, John Wiley & Sons Ltd., Oxford, U.K.

Tornqvist, T. E., T. R. Kidder, W. J. Autin, K. van der Borg, A. F. M. de Jong, C. J. W. Klerks, E. M. A. Snijders, J. E. A. Storms, R. L. van Dam, and M. C. Wiemann (1996), A revised chronology for Mississippi river subdeltas, *Science*, *273*(5282), 1693–1696.

Vail, P. R., R. M. Mitchum, and S. Thompson (1977), Seismic stratigraphy and global changes of sea level, Part 4: Global cycles of relative changes of sea level, in *AAPG Memoir 26 Seismic Stratigraphy—Applications to Hydrocarbon Exploration*, edited by C. E. Payton, pp. 83–98, American Association of Petroleum Geologists, Tulsa, OK.

Van Dijk, M., G. Postma, and M. G. Kleinhans (2009), Autocyclic behaviour of fan deltas: An analogue experimental study, *Sedimentology*, *56*(5), 1569–1589, doi:10.1111/j.1365-3091.2008.01047.x.

Van Heijst, M. W. I. M., and G. Postma (2001), Fluvial response to sea-level changes: A quantitative analogue, experimental approach, *Basin Res.*, *13*, 269–292.

Van Wagoner, J. C. (1995), Sequence stratigraphy and marine to nonmarine facies architecture of foreland basin strata, Book Cliffs, Utah, U.S.A., in *Sequence Stratigraphy of Foreland Basin Deposits: Outcrop and Subsurface Examples from the Creataceous of North America, Volume 64, American Association of Petroleum Geologists, Memoirs*, edited by J. C. Van Wagoner, and G. T. Bertram, pp. 137–223, American Association of Petroleum Geologists, Tulsa, OK.

Wang, Y., K. M. Straub, and E. A. Hajek (2011), Scale-dependent compensational stacking: An estimate of autogenic time scales in channelized sedimentary deposits, *Geology*, *39*(9), 811–814.

Zhang, Y., D. A. Benson, and B. Baeumer (2007), Predicting the tails of breakthrough curves in regional-scale alluvial systems, *Ground Water*, *45*(4), 473–484.